Computer Modelling of Lithium Formate Monohydrate§

Mark C. Wojcik and Kersti Hermansson*

Institute of Chemistry, Uppsala University, P.O. Box 531, S-75 121 Uppsala, Sweden

Wojcik, M. C. and Hermansson, K., 1987. Computer Modelling of Lithium Formate Monohydrate. – Acta Chem. Scand., Ser. A 41: 562–572.

Computer modelling of crystalline lithium formate monohydrate using static and dynamical modelling (MD computer simulation) methods, and using atom–atom effective intermolecular potentials is described. Results for a ferroelectric transition in the model and for the molecular mechanism of dehydration are presented, together with a variety of predicted and measured properties of this hydrogen-bonded crystal. The ferroelectric transition of the model produces a stable alternate crystal structure whose properties are also described.

Crystallographers normally use "thermal parameters" to model dynamical processes in crystals, even though diffraction is primarily a technique used to examine crystal structure. However, a more complete picture of molecular motion is often required to better understand dynamical crystal properties, such as structural phase transitions. In this paper we describe the molecular scale behaviour of the lithium formate monohydrate crystal as predicted by a computational model, using both static (energy minimization) and dynamical (computer simulation) modelling methods. The predicted behaviour includes a ferroelectric structural transition, and the mechanism by which dehydration occurs in this crystal is also predicted.

The basic model consists of a set of intermolecular potential functions of the atom–atom form[1] for each of the different types of molecular pair interactions. The construction of a suitable model is obviously of great importance, and a knowledge of the real crystal structure from diffraction studies can be a significant aid in this. The static modelling method involves finding the crystal structure of zero internal stress – subject to various applied external fields (mechanical, electrical etc.).[2] The second method, well known in statistical mechanics, is molecular dynamics computer simulation (MD) where, in contrast, the real-time motions of a collection of molecules are followed directly.[3,4] The effects of temperature and anharmonicity are automatically included in the MD method, while the static model corresponds, strictly speaking, to zero temperature.

Such modelling calculations complement the information gained from diffraction experiments insofar as unambiguous information about specific molecular motion and rearrangement can be obtained. We have chosen to model lithium formate monohydrate, firstly, with the aim of learning about the role of hydrogen bonds in the propagation of acoustic and optical waves, secondly, to examine the behaviour of the probability distribution functions with temperature, including full anharmonicity (assuming rigid molecules), and thirdly, to examine the mechanism by which the crystal loses water upon heating. In the present work we compare the results from the model with experimental data for acoustic velocities, normal mode frequencies and dielectric properties, and make predictions concerning the tensile strengths and the existence of a change in the spontaneous polarization in the presence of a strong electric field. The resulting, predicted new crystal structure is stable when the field is removed, and we describe some of its properties. We also present preliminary MD results for the mechanism of dehydration in the crystal. Other

§Presented at the *XII Nordiska Strukturkemistmötet* in Sånga-Säby, Sweden, June 8–13, 1987.

*To whom correspondence should be addressed.

topics mentioned above will be discussed elsewhere.

Our aim is to describe a few illustrative examples of the capabilities of these modelling methods in helping to understand the observed behaviour of matter. In section 2 we give a brief outline of the static and dynamic modelling methods. In section 3 the construction of the model potentials is discussed, and in sections 4 and 5 the new results for the model of the lithium formate monohydrate crystal are presented.

Methods

The static modelling method has been recently described by Busing and Matsui,[2] who also give a comprehensive list of references. Briefly, once the forms for the intra- and intermolecular potentials have been assumed, the equilibrium structure of the model crystal is found by adjusting the structural variables so as to minimize the total system energy. The effects of hydrostatic pressure, tensile and shear stresses, and electric fields are included by adding terms to the total energy that are appropriate to the desired effect. The total energy is minimized as above and the resulting structure reflects the effects of the applied field. In this way it is possible to calculate, for example, elastic constants, limiting tensile strengths, the bulk modulus, piezoelectric coefficients, and static dielectric constants, as described by Busing *et al.*[2]

In the MD method, one follows the classical trajectories of all the members of a collection of N molecules ($N \sim 100$–1000) by solving numerically the coupled Newton-Euler differential equations of motion that govern their individual motions.[5,6] The results is a specific trajectory of this many-body system in phase space. By the ergodic theorem, the evaluation of average mechanical properties of the system (such as energy, pressure and fluctuation properties) from the trajectory in phase space is equivalent to sampling from a statistical ensemble weighted by the many-body Boltzmann probability distribution,[7] so that the effects of temperature are rigorously introduced into the modelling. The MD method also permits study of time-dependent properties of individual molecules and of the collective behaviour of the system. This is achieved by periodically storing molecular positions, velocities, etc. during the simulation for later analysis.

The simulation begins (see, for example, Ref. 6) with an initial configuration of molecules (i.e. a lattice) and a random assignment of molecular velocities, and proceeds by stepwise solution of the coupled differential equations for translational and rotational motion. First, the force and torque acting on each molecule due to its neighbours are evaluated. The molecular positions, orientations, velocities, etc. are then predicted for the next instant of time from a Taylor expansion about the present time. The whole system is then advanced in time to the predicted configuration, velocities, etc., and the forces and torques are evaluated again. Correction factors based on the differences between predicted and evaluated forces and torques are applied to the other predicted quantities and the procedure then repeats, typically for several thousand steps using time steps of 10^{-14}–10^{-15} s.

The above is the standard predictor-corrector method used for solving differential equations, and a form due to Gear[8] has found widespread use. The evaluation of the forces is the most time-consuming part (>90 %) of the simulation because of the large number [$O(N^2/2)$] of intermolecular interactions to consider. In the present work, for example, one time step required ~4 s CPU on the Cray 1S computer in Linköping. Properties such as the pressure, energy and molecular distribution functions are readily evaluated during the calculation of the forces. The temperature is given by the kinetic energy of all the molecules, and is controlled during the "equilibration" stage of the simulation. This stage is later neglected in the study of the system properties. A flow chart of the MD algorithm is shown in Fig. 1.

In order to eliminate surface effects, which would be quite large in such small systems, it is customary to introduce periodic boundary conditions as in the static modelling, so that one is actually modelling a central "supercell" embedded in an infinite lattice of identical cells. In this way the interior of a bulk crystal is approximated. When long-range forces are present, as in ionic systems, it is necessary to use lattice summation techniques to achieve an accurate representation of the forces.[9]

Recently, a method for performing MD simulations at constant pressure and/or applied stress has been developed (see Refs. 43 and 44 in Ref. 3). This method has proven to be quite useful in

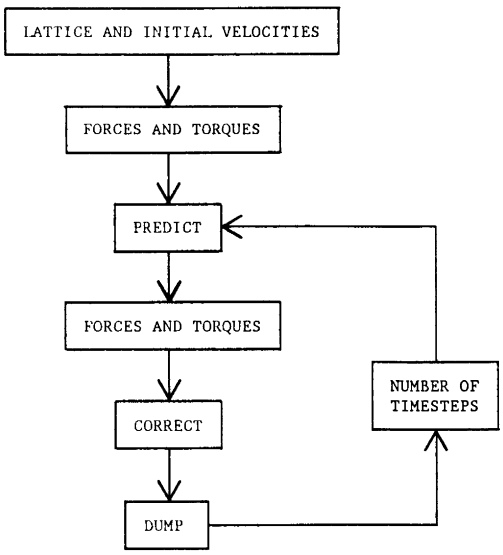

Fig. 1. Flow-chart of the MD algorithm. The evaluation of the forces takes typically about 90 % of the CPU time.

the study of pressure- and/or temperature-induced phase transitions in solids, and is the method we have used in this work. Setting the external pressure equal to zero approximates atmospheric pressure, and the system is allowed to undergo microscopic volume fluctuations which facilitate the molecular rearrangement that accompanies structural transitions.

The field of MD is too vast to discuss in more detail here, and the reader is referred to the many reviews on the subject that have appeared over the years (Refs. 3, 4, 6, 10 and 11, and references therein).

The model potential

In computer modelling of matter it is desirable to express the intermolecular forces in terms of simple analytic functions containing a few adjustable parameters. One of the more useful forms has been the atom–atom potential,[1,2] in which the potential energy $u(12)$ between a pair of molecules 1 and 2 is taken to be the sum of the interaction energies $u_{\alpha\beta}(r_{\alpha\beta})$ between the sites α on 1 and sites β on 2, and these depend only on the distance $r_{\alpha\beta}$ between sites α and β. Thus, $u(12)$ can be written as:

$$u(12) = \sum_{\alpha\beta} u_{\alpha\beta}(r_{\alpha\beta}). \tag{1}$$

The atom–atom terms typically represent overlap repulsion, van der Waals attraction and long-range electrostatic interactions in the form:

$$u_{\alpha\beta}(r_{\alpha\beta}) = A_{\alpha\beta}\, e^{-B_{\alpha\beta} r_{\alpha\beta}} - \frac{C_{\alpha\beta}}{r_{\alpha\beta}^6} + \frac{q_\alpha q_\beta}{r_{\alpha\beta}}, \tag{2}$$

where the parameters $A_{\alpha\beta}$, $B_{\alpha\beta}$, $C_{\alpha\beta}$, q_α and q_β are to be determined for a given system. In condensed matter systems many-body forces may be important, but are usually included indirectly by adjusting the parameters in the pair potentials in

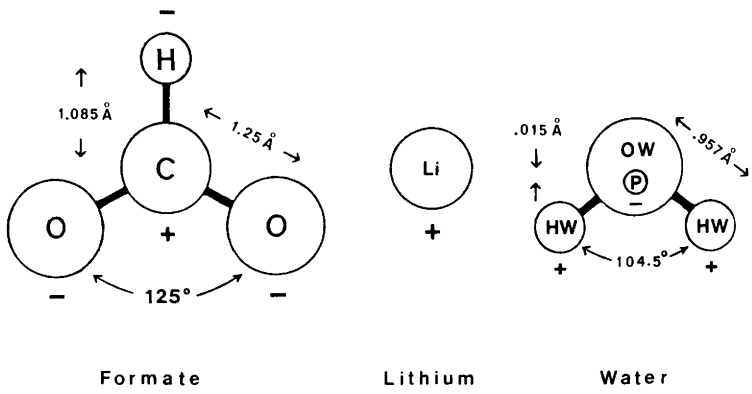

Fig. 2. Schematic diagram of the rigid model molecules. Point charges are placed on the formate, the lithium and the water hydrogen nuclei, and on the point P offset by 0.15 Å from the water oxygen toward the hydrogen atoms. For other parameters, see section 3 and Table 2.

order to give agreement with one or more experimental bulk properties.[12] This is because in practice, the evaluation of the many-body forces is too time-consuming to be carried out explicitly. Pair potentials derived in the above way are more appropriately called "effective" pair potentials. We have chosen to work with perfectly rigid model molecules with the water geometry taken from gas phase measurements[13] and with a symmetrical formate ion having C–O bond lengths of 1.25 Å, a C–H bond of 1.085 Å and an O–C–O angle of 125°. This was done for the sake of expedience, as the use of fully flexible molecules substantially increases the computing time in the MD runs. These molecules are illustrated schematically in Fig. 2. We initially experimented with a set of potentials that had been obtained from *ab initio* calculations of molecular pair energies for a large number of relative orientations and separations of the various types of pairs (WW, WL, WF, LL, LF and FF) in the lithium formate monohydrate system.[14] It was not possible to arrive at a stable crystal structure which was near to the experimental density at atmospheric pressure with these potentials. Instead, we fitted the parameters $A_{\alpha\beta}$, $B_{\alpha\beta}$, $C_{\alpha\beta}$, q_α and q_β such that the resulting model crystal structure was very close to the known structure[15] for this compound in terms of cell vectors, symmetry and intermolecular bonding distances. This was done using the program WMIN written by Busing[16] for such purposes. The water–water potential model was adopted unchanged from simulation studies of liquid water,[17] and the net charges on the lithium and formate ions were constrained to be ±1. The initial values of the remaining parameters were taken from the literature on the modelling of protein interactions[18a,*] together with the unlike pair combining rules:[12]

$$A_{\alpha\beta} = (A_{\alpha\alpha}A_{\beta\beta})^{1/2},$$
$$B_{\alpha\beta} = \tfrac{1}{2}(B_{\alpha\alpha} + B_{\beta\beta}),$$
$$C_{\alpha\beta} = (C_{\alpha\alpha}C_{\beta\beta})^{1/2}. \qquad (3)$$

By alternately adjusting the parameters and the structure to minimize the computed crystal energy we arrived at the parameters given in Table 1. Table 2 shows a comparison of bond distances and cell constants for the model and real crystals

*For an application, see Ref. 18b.

Table 1. Potential parameters for the model crystal. The van der Waals $C_{\alpha\beta}$ terms are combined according to $C_{\alpha\beta} = (C_{\alpha\alpha}C_{\beta\beta})^{1/2}$ in eqn. (2). Units are: $A_{\alpha\beta}$ in kJ mol^{-1}, $B_{\alpha\beta}$ in Å^{-1}, $C_{\alpha\alpha}{}^{1/2}$ in (kJ mol^{-1})$^{1/2}$ Å^3 and q_α in e$^+$. See also Fig. 2.

α	β	$A_{\alpha\beta}$	$B_{\alpha\beta}$
OW	OW	787167.0103	4.050551
OW	Li	4702864.0114	6.407792
OW	C	446376.2735	3.961965
OW	O	340807.9181	3.639010
OW	H	394942.8822	4.217630
Li	Li	28139917.6178	10.137875
Li	C	2669385.2252	6.268021
Li	O	2037623.2265	5.757052
Li	H	2359288.0574	6.672004
C	C	252901.5990	3.875068
C	O	193295.3861	3.559479
C	H	223724.2055	4.125072
O	O	147669.5716	3.269470
O	H	170952.7775	3.789027
H	H	198016.1089	4.391358
α		$C_{\alpha\alpha}^{1/2}$	q_α
OW		46.84400	0.00000
HW		0.00000	0.52000
P		0.00000	−1.04000
C		47.06500	0.92703
O		39.30700	−0.84706
H		10.88000	−0.23291
Li		18.96700	1.00000

at what is essentially zero pressure. The root–mean–square deviation of the nuclear positions in the model crystal is about 0.2 Å from the experimental positions. The good agreement shown in

Table 2. Intermolecular bond distances and cell vectors (Å) in the model and real lithium formate monohydrate crystals.

Bond distances	Model ($T = 0$)	Expt. (T = 300 K)
O1–OW	2.623	2.716
OW–OW	2.826	2.896
Li–O2	1.958	1.929
	1.966	1.958
Li–O1	1.931	1.933
Li–OW	1.914	1.979
Cell vectors		
a	9.572	9.984
b	6.589	6.491
c	4.842	4.852

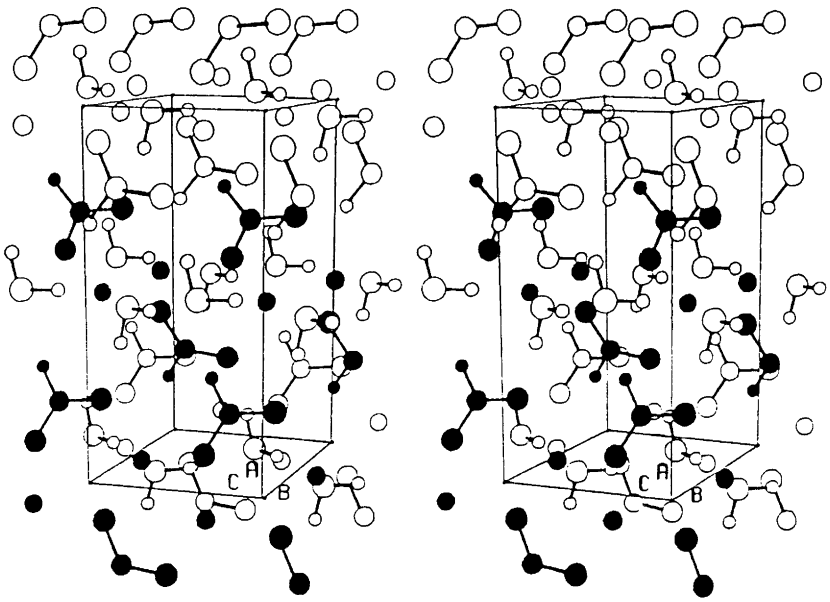

Fig. 3. Stereoscopic drawing of the model lithium formate monohydrate crystal. The atoms in the ionic backbones are darkened for contrast. The sheets are perpendicular to the *b*-axis, and are bound together through water molecules.

Table 2 and in other structural aspects is encouraging.

We cannot claim that these potentials are the optimum ones in an absolute sense because there is unavoidably a degree of arbitrariness in such fitting procedures. Rather, given the chosen form for $u(12)$ we would hope that they will represent the important features of the real system satisfactorily for our purposes. In the next section we compare some physical properties of the model crystal with experiment, and also make predictions of other properties not yet measured.

Physical properties of the static model

The model crystal minimum energy structure is shown in Fig. 3 in the same way as the neutron diffraction results[15] were presented. Here, the various sizes of the atoms are meant to denote only a difference in type and not thermal motion. Since the model and experimental structures are so close, Fig. 3 will henceforth be referred to in connection with both.

The real crystal structure is orthorhombic with space group $Pna2_1$ and with unit cell vectors as given in Table 2. The asymmetric unit consists of a formate anion, a water molecule and a lithium cation in a nearly planar arrangement, as shown in Fig. 4. The unit cell contains four asymmetric units lying roughly parallel to each other and forming "sheets" in the $a-c$ plane that are linked to each other through ion–water bonds. The lithium and formate ions interlock to form "backbones" running parallel to the *c*-axis, and between the backbones run infinite zig-zag chains of hydrogen-bonded water molecules (which also bind to the backbones). The ionic backbones are staggered, as can be seen in Fig. 3.

The acoustic properties have been measured recently[19,§] and by applying tensile and shearing loads on the model crystal, as described by Busing *et al.*,[2] the corresponding acoustic velocities can be obtained from the calculated strains. The experimental and model acoustic velocities are compared in Table 3, together with the bulk modulus. We note that the longitudinal velocity is lowest in the direction normal to the sheets (along the *b*-axis), and is highest along the *c*-axis

[§]Note that the choice of *a*, *b*- and *c*-axes in the present work and in Ref. 15 corresponds to $-b$, $-a$ and $-c$, respectively, of Ref. 19.

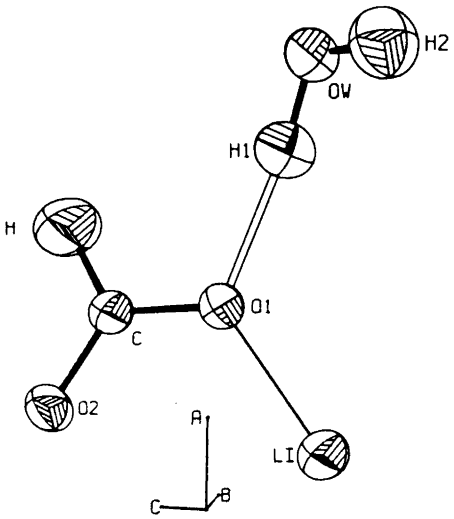

Fig. 4. Asymmetric unit of lithium formate monohydrate from Ref. 15. Four asymmetric units lie roughly parallel to each other in a staggered arrangement in the primitive unit cell.

Table 4. Properties of model and real lithium formate monohydrate crystals: P_s spontaneous polarization; ε_α° static dielectric constant along α-axis; d_{24} piezoelectric modulus; $-(\partial P_s/\partial T)_P$ pyroelectric coefficient; $\varepsilon_\alpha^\infty$ high frequency dielectric constant from index of refraction $n_\alpha^2 = \varepsilon_\alpha^\infty$ at $\lambda = 1.064$ μm.

	Model	Expt.
P_s/C m^{-2}	5.06×10^{-2}	$2\text{–}12\times10^{-2}$
ε_a°	1.5	4.7
ε_b°	1.6	5.2
ε_c°	1.9	5.0
d_{24}/C N^{-1}	27.4×10^{-12}	15.2×10^{-12}
$-(\partial P_s/\partial T)_P$/C K^{-1} m^{-2}	1.4×10^{-5}	5×10^{-7}
ε_a^∞	1	2.15
ε_b^∞	1	1.85
ε_c^∞	1	2.26

in both the model and real crystals. The shear velocities also agree well with experiment, both in order and in magnitude. The model is thus consistent with the experimental acoustic velocities and their interpretation in terms of the observed bonding scheme. Two types of bonding, ion–ion and ion–water, are important in explaining the acoustic velocities. Along the *a*- and *b*-axes the ionic backbones are held together through relatively weaker bonds to water molecules, while along the *c*-axis the stronger ionic bonds form a rigid structure that resists compression and shearing (σ_{55}, i.e. crushing).

The limiting tensile strengths for lithium formate monohydrate have not been reported to date, but predictions from the model crystal show that failure occurs first along the *b*-axis (as ex-

Table 3. Acoustic velocities (m sec^{-1}) and bulk moduli (bar) for the model and real lithium formate monohydrate crystals. The last column to the right contains results for the new crystal structure resulting from a ferroelectric transition described at the end of section 4.

Propagation direction	Shear direction	Model ($T=0$)	Experiment[a] ($T=290$ K)	New structure
100	100	4990	4794	5198
010	010	4296	3622	5465
001	001	5622	5362	5844
110	110	4438	3734	5284
001	100	3447	3207	2489
001	010	2019	1907	2380
100	010	2003	1830	1475
010	001	2019	1949	2380
101	101	2969	2648	2832
011	011	2689	2367	2677
		$K_T = -V(\partial P/\partial V)_T$		
		2.29×10^5	1.56×10^5	2.97×10^5

[a]Ref. 19.

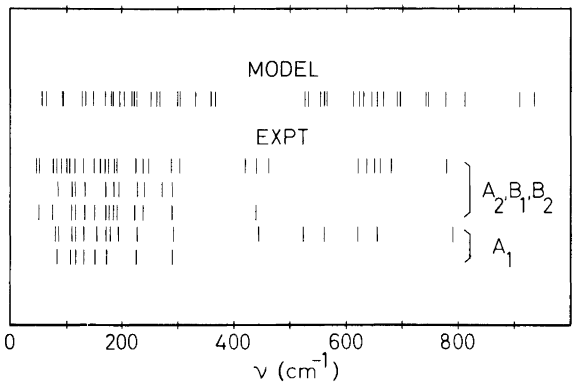

Fig. 5. Normal mode frequencies of the model crystal, and experimental IR and Raman frequencies from Refs. 21, 24. The gap in the intermediate range separates the water molecule translational and librational modes.

pected) under a load of 20 kbar, followed by failure along *a* at 33 kbar, with the ionic backbone yielding at the highest load (along *c*) of 40 kbar. At all loads less than that at which failure occurs, the crystal appears to return to the original structure upon reduction of the load. The model crystal was also subjected to hydrostatic pressure in order to investigate the possibility of a pressure-induced structural transformation. However, no such transition was found up to a pressure of 100 kbar, as was evidenced by a smoothly and reversibly varying cell volume.

The real crystal is piezoelectric and pyroelectric, with a spontaneous polarization along *c* estimated to be between 2 and 12×10^{-2} C m^{-2},[20] but it has not been shown definitively to be ferroelectric.[21] The three static dielectric constants have recently been measured,[22] as have the piezoelectric modulus[19] and the pyroelectric coefficient.[22] The indices of refraction are also known.[23] These results are summarized in Table 4.

The model crystal does not account explicitly for molecular (or electronic) polarizability, but by imposing an electric field as described in Ref. 2 it is possible to make a rough estimate of the contribution to the crystal polarizability from the ionic displacements and reorientations of the permanent molecular dipoles. The model static dielectric constants and piezoelectric coefficient obtained in this way are given in Table 4, together with the spontaneous polarization. Part of the difference between the model and experimental dielectric constants is, of course, due to the electronic polarizability. The differences are, however, of the same magnitude as those found with ionic displacement models for other ionic crystals such as NaCl, KBr, etc. The piezoelectric coefficient is somewhat less than the experimental value for the same reason. The spontaneous polarization P_s of the model is in full agreement with the estimate of Torre *et al.*[20] The pyroelectric coefficient reflects the change in P_s with temperature, and is discussed further in section 5. We note, however, the serious experimental difficulties in its measurement.[22]

The external modes (translational and librational) of the model lattice of rigid molecules can be determined in the harmonic approximation from the second derivatives of the intermolecular potentials. The normal frequencies determined in this way (using WMIN) lie typically below 1000 cm^{-1}, and they are compared with experimental IR and Raman frequencies[21,24] in Fig. 5. Identification of the particular normal modes requires a more complete group-theoretical analysis than we have carried out at present. However, through isotopic substitution in the model it is fairly straightforward to separate the specific contributions to the spectra from given molecular types or groups, and our results of this kind are in general agreement with the experimental assignments. For example, we observe approximately the same gap of ~120 cm^{-1} between water translational modes and librational modes as is found in the experimental spectra and also in the force field calculations of Eriksson and Lindgren[25] for various water molecule environments. In the present model the gap is predicted to occur ~60 cm^{-1} higher than shown by experiment (300–420 cm^{-1}). We note that although molecular polarizability is not explicitly accounted for in this model, many important features of the intermolecular motion are qualitatively reproduced. We expect that the effect of including polarizability

Table 5. Properties of the new model crystal structure (produced by ferroelectric transition) together with the ordinary model crystal. Symbols are as in Table 4.

	New crystal structure	Normal structure
a/Å	9.839	9.572
b/Å	3.433	6.589
c/Å	9.161	4.842
ε_a°	8.7	1.5
ε_b°	7.7	1.6
ε_c°	1.7	1.9
$P_s(a)$/C m^{-2}	-50.94×10^{-2}	0
$P_s(c)$/C m^{-2}	-66.58×10^{-2}	5.06×10^{-2}
d_{24}/C N^{-1}	71.2×10^{-12}	27.4×10^{-12}
d_{14}/C N^{-1}	77.8×10^{-12}	8.1×10^{-12}

would be similar to that found in simple ionic crystals, i.e. to damp higher frequency vibrations and thereby improve agreement with experiment.

There has been some question about the ferroelectricity of lithium formate monohydrate.[21] On applying a strong electric field in the direction opposite to the direction of polarization (the *c*-axis), we have found that the model crystal transforms to a different structure with markedly different dielectric constants, direction of polarization, acoustic properties, etc. At a field strength of about 50 000 kV cm^{-1}, the model crystal structure slowly and continuously changed to a new orthorhombic structure which remained stable when the field was removed. The new crystal possessed cell vectors, dielectric constants and piezoelectric coefficients as given in Table 5, and acoustic velocities as given in Table 3. The lattice energy of the new structure, -994.1 kJ mol^{-1} on a formula unit basis, is quite close to that (-1010.5 kJ mol^{-1}) of the original structure.

The new crystal structure is shown in Fig. 6. Comparison with the ordinary structure in Fig. 3 shows that the *b*-axis has collapsed to half its previous length, while *c* has increased by a factor of two. The ionic backbones of Fig. 3 are now evenly stacked; they are held together in the *b*-direction by lithium ion–water bonds, and in the *a*-direction by water molecules hydrogen-bonding to formate ions in adjacent rows. The basic symmetry is the same as before. The longitudinal sound velocity in the new crystal is lowest along the *a*-axis, as should be expected since this is the direction in which the hydrogen bonds operate. It is highest, as before, along the *c*-axis, which lies parallel to the remaining ionic backbone. A preliminary MD simulation shows that the new crystal is also stable at 300 K. The substantially larger dielectric constants and piezoelectric coefficients in Table 5 for the *a*- and *b*-directions are interesting, and suggest that if the real crystal transformed in a similar fashion it could also have interesting and possibly useful properties. At field strengths above about 75 000 kV cm^{-1} the new structure became unstable. We hope that predictions of this sort will serve as stimuli to experimental investigation.

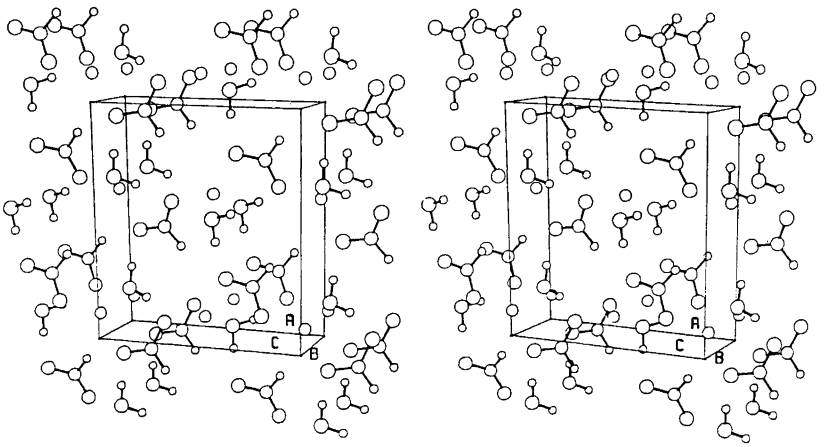

Fig. 6. Stereoscopic drawing of the new model crystal structure resulting from ferroelectric transition. See section 4.

Physical properties of the dynamic model

So far we have been discussing results for the model crystal at $T = 0$, obtained from the static calculations. These are valuable checks on the potentials and provide confidence that we can learn something that is relevant to the real crystal when temperature effects are included. To introduce temperature effects correctly it is necessary to use computer simulation methods such as MD. In this work we have included 24 crystallographic unit cells in the system (288 molecules) and used periodic boundary conditions for this supercell, together with Ewald summation for the long-range electrostatic forces and a generalized lattice summation[26] for the r^{-6} terms. After the temperature had stabilized to the desired value during the equilibration stage (typically a few picoseconds), the trajectories were stored on magnetic tape for later study. The simulations themselves were continued long enough for statistically meaningful results to be obtained for the time-dependent properties (from 4 ps at low temperature to 10 ps at higher temperatures), care being taken that the conservation laws of mechanics were being obeyed (see Ref. 3). The external pressure was always maintained at zero (≈ atmospheric pressure). The results of these simulations include, among other things, the average structure, mean-square amplitudes, average single-molecule motion, average collective motion (like phonons, and IR and Raman bands) and their temperature dependences.

Lithium formate monohydrate begins losing water in air at ~47 °C and at ~87 °C when the crystal surface is sealed with a hydrophobic medium such as transformer oil.[27] The latter situation is closer to that of the simulation model in that water molecules are not free to escape from the system. Yuzvak *et al.*[27] observed the appearance of a liquid-like component in the Li^7 NMR spectrum at 87 °C and speculated that its occurrence may be due to the partial solvation of the lithium ions by water molecules. Clearly, the MD method offers the means to examine the detailed mechanism by which this happens.

We have performed a series of exploratory runs at 50 K, 150 K, 300 K, 500 K and 700 K. The simulation results show that the unit cell volume increases slowly and nearly linearly up to about 300 K, and then increases considerably more rapidly beyond about 400 K. This is shown in Fig. 7. Between 500 K and 700 K both the *a* and *b* cell vectors were found to increase by 1 Å each, which means that the spacing between the ionic backbones has increased, i.e. the water molecules no longer bind the sheets together at 700 K. The *c* cell vector remained unchanged during the temperature increase, presumably be-

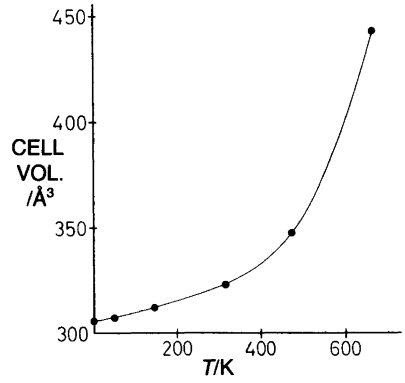

Fig. 7. Temperature variation of the model crystal cell volume from MD simulations. There is a sharp increase with temperature beyond about 400 K.

Table 6. Temperature variation of mean-square force on a water molecule along its principal directions (see text), and mean-square torques on water and formate molecules (about the principal axes).

	T/K				
	50	150	300	500	700
Mean-square force (water)/10^{-19} N^2					
xx	0.62	1.42	2.64	3.07	3.00
yy	0.32	0.91	1.76	2.25	2.86
zz	0.60	1.53	3.35	5.16	6.25
Mean-square torque (water)/10^{-39} J^2					
xx	0.36	0.93	1.70	1.85	1.78
yy	0.19	0.43	0.81	0.96	0.94
zz	0.31	0.70	1.27	1.24	0.93
Mean-square torque (formate)/10^{-39} J^2					
xx	2.35	5.35	10.21	12.97	13.59
yy	0.14	0.50	0.79	1.10	1.42
zz	0.72	2.23	4.67	7.02	9.66

Table 7. Temperature variation of spontaneous polarization in the model lithium formate monohydrate crystal. The direction of polarization at 700 K is midway between the *a*- and *b*-axes in the *a*–*b* plane, and lies along the *c*-axis at the lower temperatures.

Spontaneous polarization /10^{-2} C m^{-2}	*T*/K				
	50	150	300	500	700
Total	4.99	4.90	4.54	4.82	6.44
Water dipoles	−4.65	−4.37	−3.74	−0.28	~0

cause of the absence of water molecules in the interlocking ionic structure forming the backbones.

Table 6 shows the temperature variation of the mean-square force on the water molecules in the *xx*, *yy* and *zz* directions (normal to the molecular plane, in the plane and normal to the symmetry (*z*) axis, and along the symmetry axis, respectively). At 50 K the values reflect essentially the intermolecular bonding in the static lattice ($T = 0$), that is, for an average water molecule, one strong hydrogen bond to the formate ion and one ion–water bond to the lithium ion, plus hydrogen bonds to the two neighbouring water molecules. As the temperature increases, the relative magnitudes change slowly up to 300 K, with the *xx* and *zz* components being closest in magnitude. Above 300 K the *xx* and *yy* components become similar, and both are much smaller than the *zz* component. The large *zz* component is characteristic of a water–lithium bond (i.e. the lone-pair direction toward the lithium), and the rough equality of the *xx* and *yy* forces strongly suggests that many of the water molecules are close to the lithium ions and are not otherwise strongly bound. The variation of the mean-square torques shows the same trend (see Table 6). Also, the mean-square torques for the formate ion show that it is held more rigidly at the high temperatures. The lithium and formate ions do not migrate since their mean-square displacements remain small and constant with time, but the water molecules were observed to move, on average, more than 3 Å in 4.5 ps at 700 K.

The variation of the spontaneous polarization with temperature shown in Table 7 shows the expected slow decrease in P_s as T is increased up to about 300 K, yielding the pyroelectric coefficient given in Table 4. However, at 500 K the contribution to P_s from the water molecule dipole moments drops to 10 % of that at 300 K, indicating a change in the bonding of the water molecules. The increase in P_s (and also change in direction) that follows with temperature reflects the changing structure and the dominance of the ionic components in the new structure.

The picture that emerges is that the water molecules that formed the zig-zag chains have shaken themselves loose from their hydrogen-bonded neighbours due to their increased thermal energy, thereby allowing the ionic backbones to move apart. The water molecules are then able to migrate and are sometimes temporarily "captured" by a lithium ion in the lithium–formate ionic networks. The much stronger ionic bonds remain, and the resulting expanded crystal structure can then permit water molecules to move about and presumably escape. The appearance of the liquid-like peaks in the ^{7}Li NMR spectra of Ref. 27 follows naturally from this description. A more detailed analysis based on the trajectories stored on tape will be presented elsewhere.

With the present model we have been simulating a bulk phase, and consequently there is nowhere for the water molecules to escape to. The presence of a surface and the removal of water molecules from the crystal structure introduce new features whose importance can, in principle, also be studied by MD. We are planning to introduce a free surface in future studies. Further details and an analysis along the lines described in the beginning of this section will be reported elsewhere.

Conclusions

We have tried to illustrate the usefulness of computer modelling of complicated molecular solids through the example of lithium formate monohydrate. The results for the mechanism of de-

hydration yield a molecular-level description of this process, which can be studied only indirectly by experiment. The prediction of a ferroelectric transition in this model crystal, although the applied field is large by comparison with the fields commonly used in practice, suggests a need for further experimental investigation of possible alternate crystal structures. With computer time becoming more readily available, exploratory and predictive calculations of the type presented here should play a more important role in chemistry, as they have in physics.

Acknowledgements. We would like to thank Professor I. Olovsson for the facilities he has placed at our disposal. This work has been supported by grants from the Swedish Natural Science Research Council, which are hereby gratefully acknowledged.

References

1. Califano, S., Schettino, V. and Neto, N. *Lattice Dynamics of Molecular Crystals,* Lecture Notes in Chemistry 26, Springer-Verlag, Berlin 1981.
2. Busing, W. R. and Matsui, M. *Acta Crystallogr., Sect. A 40* (1984) 532.
3. Klein, M. L. *Ann. Rev. Phys. Chem. 36* (1985) 525.
4. Lykos, P., Ed., *Computer Modelling of Matter,* ACS Symposium Series No. 86, ACS, Washington D.C. 1978.
5. Rahman, A. and Stillinger, F. H. *J. Chem. Phys. 55* (1971) 3336; Evans, D. J. and Murad, S. *Mol. Phys. 34* (1977) 327.
6. Wood, D. W. In: Franks, F., Ed., *Water – A Comprehensive Treatise,* Plenum Press, New York 1979, Vol. 6.
7. Rahman, A. *Phys. Rev. A 136* (1964) 405.
8. Gear, C. W. *Numerical Initial Value Problems in Ordinary Differential Equations,* Prentice Hall, Englewood Cliffs 1971.
9. DeLeeuw, S. W., Perram, J. W. and Smith, E. R. *Proc. Roy. Soc. London A 373* (1980) 27; *Ibid.* 57; Anastasio, N. and Fincham, D. *Comput. Phys. Commun. 25* (1982) 159.
10. Wood, W. W. and Erpenbeck, J. J. *Ann. Rev. Phys. Chem. 27* (1976) 319.
11. Kushick, J. and Berne, B. J. In: Berne, B. J., Ed., *Modern Theoretical Chemistry: Part B,* Plenum Press, New York 1977, Vol. 6.
12. Mason, E. A. and Monchick, L. *Adv. Chem. Phys. 12* (1967) 329.
13. Benedict, W. S., Gailar, N. and Plyler, E. K. *J. Chem. Phys. 24* (1956) 1139.
14. Hermansson, K., Lie, G. C. and Clementi, E. *Theor. Chim. Acta. Submitted for publication.*
15. Tellgren, R., Ramanujam, P. S. and Liminga, R. *Ferroelectrics 6* (1974) 191.
16. Busing, W. R. *WMIN.* Report ORNL-5747, Oak Ridge National Laboratory, Oak Ridge, TN 1981.
17. Jorgensen, W. L., Chandrasekhar, J., Madura, J. D., Impey, R. W. and Klein, M. L. *J. Chem. Phys. 79* (1983) 926.
18. (a) Weiner, S. J., Kollman, P. A., Case, D. A., Singh, U. C., Ghio, C., Alagona, G., Profeta, S. and Weiner, P. *J. Am. Chem. Soc. 106* (1984) 765; (b) Alagona, G., Ghio, C. and Kollman, P. *J. Am. Chem. Soc. 108* (1986) 195.
19. Zaitseva, M. P., Shabanova, L. A., Kidyarov, B. I., Kokorin, Yu. I. and Burkov, S. I. *Kristallografiya 28* (1983) 741 [Engl. transl.: *Soviet Phys. Crystallogr. 28* (1984) 439].
20. Torre, L. P., Abrahams, S. C. and Bernstein, J. L. *Proceedings of the A.C.A. Summer Meeting, Ames, Iowa 1971,* p. 94.
21. Galzerani, J. C., Srivastava, R., Katiyar, R. S. and Porto, S. P. S. *J. Raman. Spectrosc. 6* (1977) 174.
22. Pykacz, H. *Acta Phys. Pol. A 55* (1979) 855.
23. Singh, S., Bonner, W. A., Potopowicz, J. R. and Van Uitert, L. G. *Appl. Phys. Lett. 17* (1970) 292.
24. Hase, Y. *Spectrochim. Acta, Part A 37* (1981) 275; Hase, Y. *Monatsh. Chem. 113* (1982) 409; Polivanov, Yu. N. and Prokhorov, K. A. *Fiz. Tverd. Tela 22* (1980) 1316 [Engl. transl.: *Soviet Phys. Solid State 22* (1980) 768]; Agarwal, A., Khandelwal, D. P. and Bist, H. D. *Can. J. Chem. 61* (1983) 2282.
25. Eriksson, A. and Lindgren, J. *J. Mol. Struct. 48* (1978) 417.
26. Williams, D. E. *Acta Crystallogr., Sect. A 27* (1971) 452.
27. Yuzvak, V. I., Kuznetzova, L. I., Rez, I. S. and Aleksandrova, I. P. *Kristallografiya 22* (1976) 106 [English transl.: *Soviet Phys. Crystallogr. 22* (1977) 59].

Received September 4, 1987.